25th ABCM International Congress of Mechanical Engineering
October 20-25, 2019, Uberlândia, MG, Brazil

COB-2019-0867
CUTTING FORCES IN HIGH FEED MILLING

Rodrigo Oliveira Henz
Departamento de Engenharia Mecânica, Escola Politécnica, Universidade Federal do Rio de Janeiro, Brazil
rodrigo.henz@poli.ufrj.br
Guillaume Fromentin
LaBoMaP, Arts et Metiers ParisTech, Rue Porte de Paris, 71250 Cluny, France
fromentin@ensam.eu
Anna Carla Araujo
Departamento de Engenharia Mecânica Poli/COPPE, Universidade Federal do Rio de Janeiro, Brazil
anna@poli.ufrj.br
Fábio de Oliveira Campos
Departamento de Engenharia Mecânica, Centro Federal de Educação Tecnológica Celso Suckow da Fonseca — RJ, Nova Iguaçu, Brazil
fo.campos@mecanica.coppe.ufrj.br

Abstract. *This article compares the machining forces of face milling processes using inserts with same reference code used in two different tool holders: a regular feed rate holder with cutting angle of* 45^o *and a tool holder with high feed using* 15^o*. For comparison, a design of experiments with the same cutting speed, chip load area, maximum chip thickness and, consequently, different feed rates are carried out. During the machining of titanium alloy Ti6Al4V the machining forces and the angular position of the tool are collected. The model used for cutting force prediction considers the contribution of the chip load area and the cutting edge length. Tool wear is measured to confirm if it can be neglected in the model. The comparison suggests that the position angle had no impact on the force model and is economically advantageous by reducing the machining time with the same chip removal rate.*

Keywords: *Cutting force, Face milling, Titanium Alloy.*

1. INTRODUCTION

Face milling is widely used in the early operations of a machining design and is therefore a focus of study on the prediction of forces, vibrations and wear to improve process quality, optimize the machining path and mainly reduce the machining cost. Facing can eliminate other processes and, because it has a more robust tool, it has greater the capacity to remove material with less vibration and better finishing.

High-feed milling aims to remove the highest chip rate in the shortest possible time (Gylienė and Eidukynas, 2016). It is the first choice for machining applications in parts with a large area, for example in mold and die milling applications. It is a process that has existed for some time but the evolution of tool materials has meant that the lifetime of this application has been expanded (Borysenko *et al.*, 2019). In addition, machine tools must be stiffer and reach speeds much greater than those typically used. The tool holder positions the inserts in a low position to remove thinner and wider chips.

Different models were developed for the calculation of machining forces in milling, from Martellotti (1975) to Matsumura and Tamura (Matsumura and Tamura, 2017). Manufacturers claim that radial forces during face milling with high feed are larger, causing vibration and stress in the spindle bearings. Therefore, it is important to predict machining forces in this process to understand the mechanical limitation of the feed.

This paper studies the forces in face milling in two situations: with high feed geometry and regular case, predicted and experimental data area compared. The study is carried out in a low machinability part, in titanium alloy Ti6Al4V, in which increased productivity is also limited by tool wear (Arrazola *et al.*, 2009).

2. CUTTING FORCE MODELLING

The model of machining forces used in this work was initially presented by Armarego and Deshpande (Armarego and Epp, 1970; Armarego and Deshpande, 1991) and it considers that there is one parcel dependent on the chip load area and one proportional to cutting edge lenght. Each small portion of the cutting edge has length db and chip thickness h and the machining force component i depends on the specific cutting energies k_{ic} and k_{ie} (Dorlin *et al.*, 2015):

$$dF_i = k_{ic}.h.db + k_{ie}.db \tag{1}$$

As a result, the resultant force is the sum of all dF contributions: F_c in the cutting direction, F_e on the edge direction and F_h perpendicular to the cutting edge in the rake face, where h is measured. (as shown in Figure 1a).

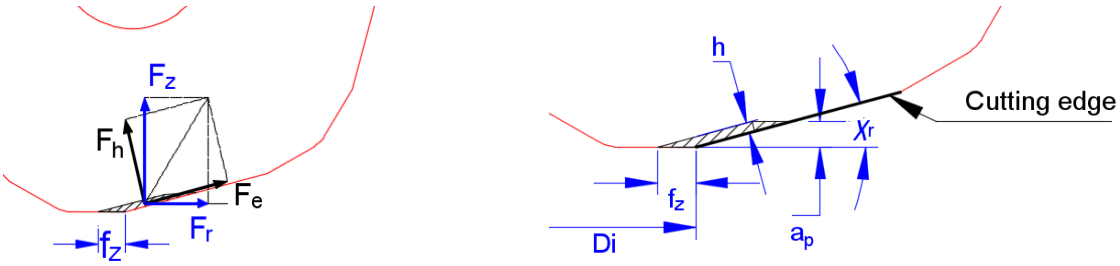

(a) Cutting force components (b) Chip geometry

Figure 1. Cutting force model

The geometry of the chip in face milling is shown in Figure 1b, considering the chip thickness does not vary along the cutting edge. In this article the inclination angle will be neglected and therefore it is assumed that the figure shows the output surface in true magnitude. Thus:

$$\vec{F_u} = \begin{bmatrix} F_c \\ F_e \\ F_h \end{bmatrix} = \int_0^b \begin{bmatrix} k_{cc} \\ k_{ec} \\ k_{hc} \end{bmatrix} h db + \int_0^b \begin{bmatrix} k_{ce} \\ k_{ee} \\ k_{he} \end{bmatrix} db = \begin{bmatrix} k_{cc} \\ k_{ec} \\ k_{hc} \end{bmatrix} hb + \begin{bmatrix} k_{ce} \\ k_{ee} \\ k_{he} \end{bmatrix} b \tag{2}$$

In order to calculate the tangential components F_t, radial F_r and vertical forces F_z on the insert reference and the spindle tool axis oriented by the cutting angle χ_r by making a reference frame (Fig. 1):

$$\vec{F_u} = \begin{bmatrix} F_c \\ F_e \\ F_h \end{bmatrix} = \begin{bmatrix} 1 & 0 & 0 \\ 0 & \cos(\chi_r) & \sin(\chi_r) \\ 0 & -\sin(\chi_r) & \cos(\chi_r) \end{bmatrix} \begin{bmatrix} F_t \\ F_r \\ F_z \end{bmatrix} \tag{3}$$

The local referential is used for modelling the forces and the workpiece referential for experimental data acquisition.

3. MATERIALS AND METHODS

3.1 Machine-tool, tool and experimental set-up

The machine-tool is a CNC DMC65V using soluble cutting fluid. In order to compare the geometry used on high feed milling (HFM) with the regular one, inserts with same reference code used in two different tool holders: for HFM $\chi_r = 15^o$ and for regular feed rate, $\chi_r = 45^o$. As the two tool holders could use 3 and 5 inserts at the same time, respectively, only one insert is used in both cases (Fig. 2 a and b). The inclination angle is the same in both cases: $\lambda = 7^o$.

The carbide insert used is indicated by the supplier for Titanium alloys (code: NPJ0604ANSNGD-KC522M). The machined workpiece is a Ti6Al4V block fixed in a Kistler dynamometer (9255), as shown in Fig. 3. The acquisition rate for A/D data conversion in cutting forces was 1kHz.

The components of the experimental force are oriented by the machine-tool coordinates x, y, z. The coordinate transformation for the cylindrical coordinates t, r, z fixed in the insert used the angular position θ of the insert, which is collected on the analog out-put of the machine-tool.

$$\begin{bmatrix} F_t \\ F_r \\ F_z \end{bmatrix} = \begin{bmatrix} \cos(\theta) & \sin(\theta) & 0 \\ \sin(\theta) & -\cos(\theta) & 0 \\ 0 & 0 & 1 \end{bmatrix} \begin{bmatrix} F_x \\ F_y \\ F_z \end{bmatrix}_{exp.} \tag{4}$$

3.2 Design of Experiments

The design of experiments is presented on Table 1. It can be seen that the values of feed and depth of cut were chosen so that the chip thickness and area were the same and could be compared, with constant cutting speed.

(a) $\chi_r = 15^o$

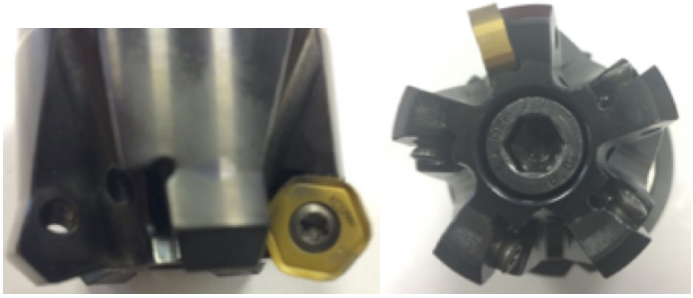

(b) $\chi_r = 45^o$

Figure 2. Tool holders

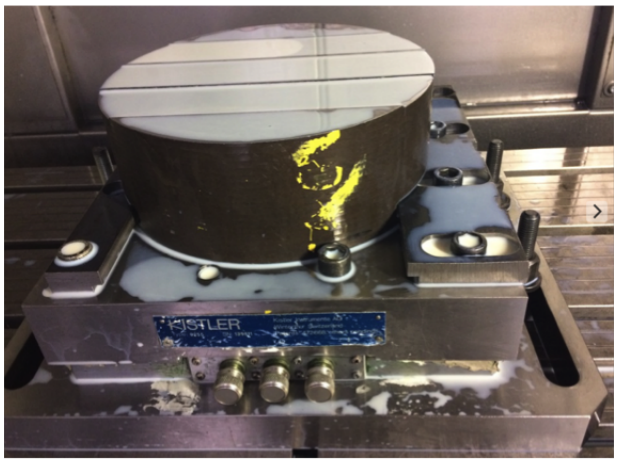

Figure 3. Workpiece fixed in the dynamometer

Table 1. Design of Experiments using $V_c = 50$ m/min

Exp. (2 replicates each)	1	2	3	4	5	6	7	8
f_t (mm)	0.3	0.6	0.3	0.6	0.11	0.22	0.11	0.22
a_p (mm)	0.4		0.6		1.1		1.65	
χ_r (deg.)	15				45			
D_i (mm)	32				40			
h (mm)	0.078	0.155	0.078	0.155	0.078	0.155	0.078	0.155
A_c (mm^2)	0.12	0.24	0.18	0.36	0.12	0.24	0.18	0.36

3.3 Cutting profile analysis

With the insert positioned in the tool holder, a profilometer was used to verify the geometry of the tool in relation to the vertical axis of the holder, mainly to identify the lateral position angle. Figure 4 shows the profiles of the profilometer as well as a detail of the dimensions of the cutting geometry. It can be seen that, although the manufacturer reports the position angle of $\chi_r = 45^o$, there is a portion of the cutting edge with position angle of $\chi_r = 30^o$. In this way, the thickness of the chip as well as the length of the edge were recalculated considering the actual geometry.

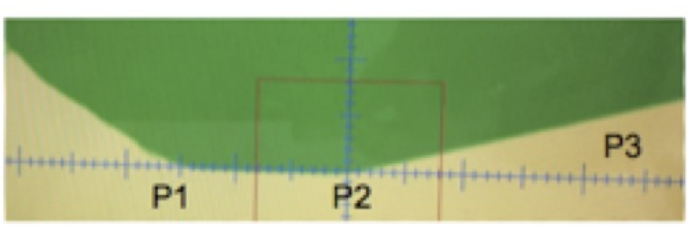

(a) Tool profile ($\chi = 15^o$)

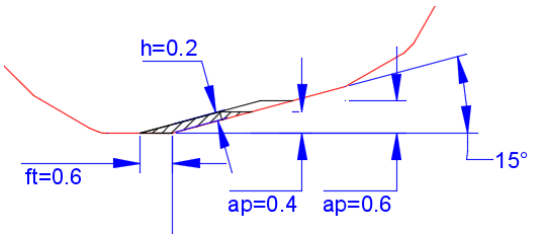

(b) Geometry with $\chi = 15^o$

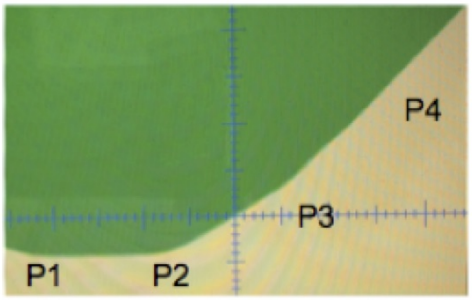

(c) Tool profile ($\chi = 45^o$)

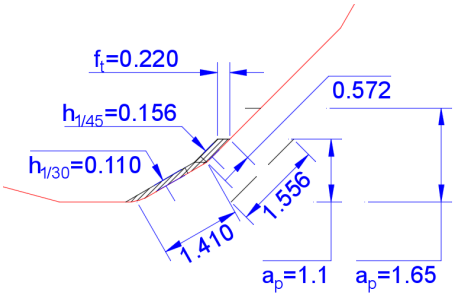

(d) Geometry with $\chi = 45^o$

Figure 4. Cutting geometry used on experiments

As the force depends on two unknown coefficients, by using data of the specific cutting force with all other known parameters, k_c and k_e are calculated separately for different κ_r experiments:

$$\frac{F}{b} = k_c.h + k_e \tag{5}$$

As the tool profile that suppose to be 45^o is actually a combination of 30^o and 45^o, an average is done considering proportional chip load:

$$F_{\chi_1} = \frac{F b_{\chi_1}}{b_{\chi_1} + b_{\chi_2}} \tag{6}$$

$$F_{\chi_2} = \frac{F b_{\chi_2}}{b_{\chi_1} + b_{\chi_2}} \tag{7}$$

4. RESULTS

4.1 Cutting Forces

The experimental results of each of the 16 tests were treated as follows: identification of the useful part of the signal (without considering entering and leaving the piece), calculation of the forces t, r, z and analysis of these as a function of the angle of rotation and calculation of the average force at the position of maximum thickness (when F_r is aligned with the feed direction).

Figure 5 presents two examples (one replica of Exp. 1 and Exp. 5) of the force curves as a function of the angular position angle. The dots represent the means of several data taken on the same angular position and the red curve the uncertainty using the standard deviation of these data. Note that the vertical force exhibits a large uncertainty, partly by the drift of the dynamometer, of the order of $0.2N/mm$.

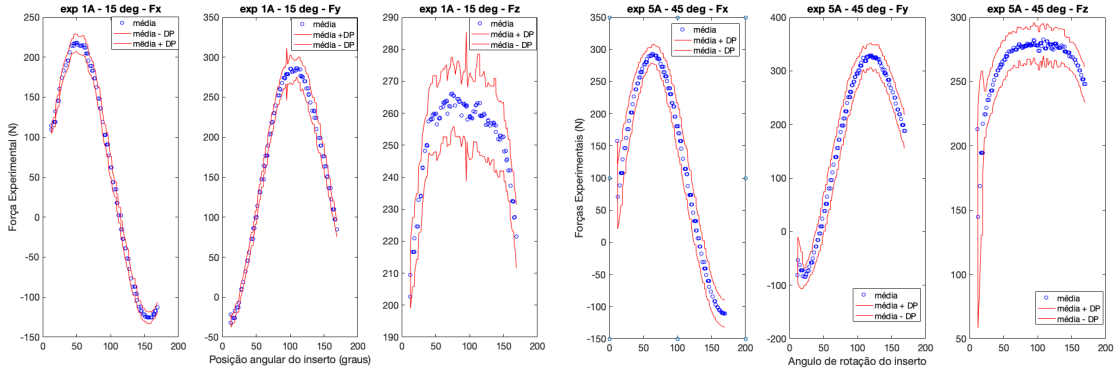

(a) Exp. 1 - 15^o (b) Exp. 5 - 45^o

Figure 5. Example of results as a function of rotation angle with uncertainty

5. Specific Cutting Forces

With all the results, all mean values of the forces in the reference frame c, h, and e were calculated using experiments 1 to 4, which constant position angle. The specific energy coefficients k_e and k_c were calibrated, as can be seen in Fig. 5a, whose calibration values are shown in Eq. 5. From these values, the theoretical forces for the experiments 5 to 8 were calculated using the geometry analyzed.

Table 2. Specific cutting forces values for all experiments and their standard deviation

Edges	$\chi_r = 15^o$	$\chi_r = Eq$	$\chi_r = 30^o$	$\chi_r = 45^o$
$K_{c,c}$	1450.9	1446.6	1601.1	1275.4
STD $K_{c,c}$	147	254	163.4	97.9
$k_{c,e}$	52.9	51.8	49.2	55
STD $k_{c,e}$	6	4.6	3.1	1.5
$K_{e,c}$	719.7	729.7	844.5	583.8
STD $K_{e,c}$	56.5	135.6	106.5	35.2
$k_{e,e}$	71	143.9	134.8	153.2
STD $k_{e,e}$	5.3	15.3	8.4	6.8
$K_{h,c}$	248	-113	-61	-196
STD $K_{h,c}$	9.7	159.6	107.2	54.1
$k_{h,e}$	125.7	60.6	75.1	36.6
STD $k_{h,e}$	3.4	9.5	7	2.4

The results of the experimental and theoretical comparison of these experiments for the cutting force F_c are shown in Fig. 6. It is observed that the prediction using the specific energy calculated with the HFM position was underestimated in the results with lower depth of cut and overestimated in the cases with $a_p = 1.65$ mm, with a maximum error of 15 %.

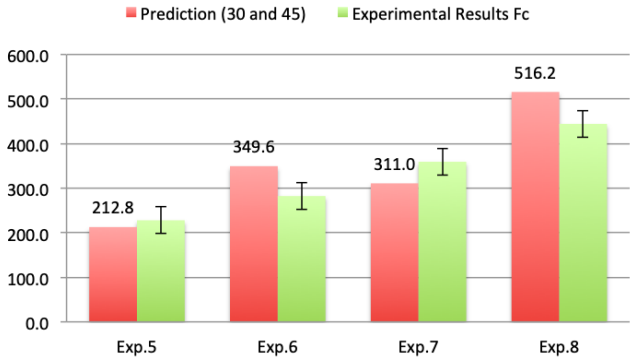

Figure 6. Experimental Validation

6. CONCLUSIONS

This article presents a theoretical and experimental comparison of cutting forces in Titanium alloy using the same carbide tool with two different cutting angles, 15^o and 45^o. Using the specific cutting energy obtained with HFM (constant cutting angle) a prediction of forces with the regular suporte is done.

The comparison showed some difference in the force components e and h, due to a experiment drift in F_z. On the other hand, the results for the c components were satisfactory, especially for small and medium contact angles. This proves that the specific cutting and edge energy is independent of the position angle.

Therefore, it is safe to assume that the theoretical values found for the e component are coherent than the experimental ones, and that just like the c component must be an approximation of the actual efforts exerted during the experiments. This is because this component depends on a smaller portion of F_z, since the position angle is smaller and so is its sine. Although there is not a good parameter to use as a comparison, theoretical data have sufficient credibility and can be used to make a forceful prediction according to this component, although not as accurate as c.

7. REFERENCES

Armarego, E. and Deshpande, N., 1991. "Computerized end-milling force predictions with cutting models allowing for eccentricity and cutter deflections". *CIRP Annals*, Vol. 40, No. 1, pp. 25 – 29.

Armarego, E. and Epp, C., 1970. "An investigation of zero helix peripheral up-milling". *International Journal of Machine Tool Design and Research*, Vol. 10, No. 2, pp. 273 – 291.

Arrazola, P., Garay, A., Iriarte, L., Armendia, M., Marya, S. and Maître, F.L., 2009. "Machinability of titanium alloys (ti6al4v and ti555.3)". *Journal of Materials Processing Technology*, Vol. 209 (5), p. 2223 – 2230.

Borysenko, D., Karpuschewski, B., Welzel, F., Kundrák, J. and Felhő, C., 2019. "Influence of cutting ratio and tool macro geometry on process characteristics and workpiece conditions in face milling". *CIRP Journal of Manufacturing Science and Technology*.

Dorlin, T., Fromentin, G. and Costes, J.P., 2015. "Analysis and modelling of the contact radius effect on the cutting forces in cylindrical and face turning of ti6al4v titanium alloy". *Procedia CIRP*, Vol. 31, pp. 185 – 190. 15th CIRP Conference on Modelling of Machining Operations (15th CMMO).

Gylienė, V. and Eidukynas, V., 2016. "The numerical analysis of cutting forces in high feed face milling, assuming the milling tool geometry". *Procedia CIRP*, Vol. 46, pp. 436 – 439. 7th HPC 2016 – CIRP Conference on High Performance Cutting.

Matsumura, T. and Tamura, S., 2017. "Cutting force model in milling with cutter runout". *Procedia CIRP*, Vol. 58, pp. 566 – 571. 16th CIRP Conference on Modelling of Machining Operations (16th CIRP CMMO).

8. RESPONSIBILITY NOTICE

The authors are the only responsible for the printed material included in this paper.